Polymer Chemistry

ROYAL SOCIETY OF CHEMISTRY

PAPER

View Article Online
View Journal | View Issue

Cite this: *Polym. Chem.*, 2025, **16**, 3857

Stereogenic-at-silicon hybrid conjugated polymers†

Qifeng Jiang,‡ Marissa G. Coschigano, Braden A. Mediavilla, Alexandra F. Gittens, Sophia J. Melvin and Rebekka S. Klausen *

Stereoregularity in carbon-based polymers impacts critical physical properties such as crystallinity, but achieving comparable precision in polysilanes remains challenging. Herein, we report the synthesis of hybrid σ,π-conjugated polysilanes with defined stereoregularity, derived from *cis*- and *trans*-cyclosilane building blocks. Using Kumada polycondensation, we accessed a series of atactic, *trans*-enriched, and *cis*-enriched polysilanes, enabling a systematic investigation of how tacticity influences thermal and optical properties. Differential scanning calorimetry revealed distinct glass transition behaviors for stereoregular polymers compared to their atactic counterpart, and UV-vis spectroscopy demonstrated enhanced spectral resolution upon annealing of stereoregular films. A linear silane-based analog further underscored the structural impact of cyclic stereogenic units. These findings highlight how stereochemical precision in silicon-containing backbones can modulate macromolecular properties, opening avenues for the rational design of stereoregular polysilanes.

Received 24th April 2025,
Accepted 22nd July 2025

DOI: 10.1039/d5py00405e

rsc.li/polymers

Introduction

Stereoregular polymers have pronounced differences in thermal, mechanical and other properties relative to atactic polymers.[1] While the synthesis of stereoregular polyolefins has been extensively studied,[2] the stereoregular synthesis of polymers with cyclic repeating units in the main chain requires distinct synthetic approaches. Polysaccharides are highly stereoregular natural and synthetic macromolecules with cyclic repeat units in the main chain.[3–11] Some linear α,ω-dienes undergo a coordination–insertion cyclopolymerization to form 5- or 6-membered rings fused to the polymer backbone.[12–14] Takeuchi reported a precise isomerization polymerization of alkenylcyclohexanes yielding stereoregular polymers containing six-membered rings in the polymer backbone.[15,16] An alternative approach is to polymerize a monomer with predefined configuration, for example, the ring-opening polymerization of one ring in a polycyclic monomer can proceed with retention of configuration at the ring-fusion.[17–21]

In recent years, we have described the synthesis of poly(cyclosilane)s, macromolecules with all-silicon backbones and constitutional repeat units based on a cyclohexasilane.[22–28] ^{29}Si NMR studies and computational modeling show that the poly(cyclosilane)s are tactic materials, with two distinct stereoisomers in a *ca.* 2 : 1 ratio.[28,29] We have attempted the stereoselective dehydropolymerization of cyclosilanes, although zero to low conversion was observed (Fig. S1†). In contrast to carbon-based macromolecules, control of tacticity in polysilanes is a challenge with respect to both analysis and synthesis. Monomers with two different side chains (*e.g.*, $Cl_2SiR^1R^2$ or $H_2SiR^1R^2$) will result in each silicon atom in the chain being a stereogenic center. Efforts to characterize poly(SiMePh) tacticity and assign ^{29}Si NMR resonances to specific triads have resulted in conflicting conclusions. Schilling *et al.* assigned the structure of poly(SiMePh) to an atactic polymer (mm : mr : rr = 1 : 2 : 1),[30] while Maxka *et al.* reported a 3 : 4 : 3 assignment inconsistent with Bernouillian statistics.[31–33] A lack of stereochemically well-defined small molecule model systems,[34] such as those employed in the assignment of polyolefin NMR resonances,[35,36] contributes to the characterization challenge, which has also been noted in poly(SiHR) materials arising from dehydropolymerization.[37–41]

The clearest evidence for polysilane main chain stereoselectivity arises from anionic ring-opening polymerization (ROP). Matyjaszewski reported the ROP of an all-*trans* cyclotetrasilane resulting in a polysilane enriched in isotactic sequences (Fig. 1a), an assignment supported by careful comparison of the poly(SiMePh) to pure stereoisomers of the starting cyclotetrasilane.[42,43] Sakurai reported that anionic ROP of amino-functionalized masked disilenes yielded a syndiotactic polysilane.[44]

Department of Chemistry, Johns Hopkins University, 3400 N. Charles St, Baltimore, MD 21218, USA. E-mail: klausen@jhu.edu

†Electronic supplementary information (ESI) available. See DOI: https://doi.org/10.1039/d5py00405e

‡Present address: Department of Chemistry, Columbia University, New York, New York 10027, United States.

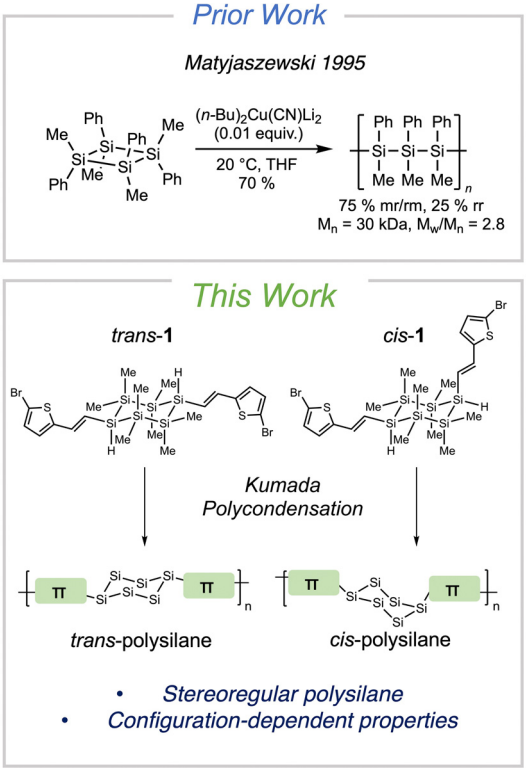

Fig. 1 Prior Work: Ring-opening polymerization of an all-trans cyclotetrasilane. This work: Stereoregular polysilane synthesized from cyclosilane building blocks.

Towards the dual challenge of characterizing and controlling polysilane tacticity, we pursued the stereocontrolled synthesis of small molecules possessing *cis*/*trans* stereoisomerism, Si–Si bonds, and reactive sites potentially suitable for polymerization.[28,45–47] We recently described highly chemo- and regioselective $RuHCl(CO)(PPh_3)_3$-catalyzed[48] hydrosilylation reactions between aryl alkynes and cyclosilanes.[47] The resulting molecules exhibit σ,π-conjugation, as supported by red-shifted absorbance relative to purely σ-conjugated cyclosilanes and purely π-conjugated styrene. The product of this reaction is a σ,π-hybrid conjugated molecule that has two silicon-centered stereogenic centers and exists as typically a *ca.* 2 : 1 mixture enriched in the *trans* diastereomer. The *trans* diastereomer can be further purified by recrystallization, allowing access to both stereoisomers and facilitating assignment of specific NMR resonances to each isomer. Other conjugated materials have been previously reported, but without stereogenic centers.[49–51]

Herein, we report the synthesis of atactic, *trans*-enriched, and *cis*-enriched polysilanes derived from the polymerization of mixtures or pure samples of diastereomeric building blocks (Fig. 1b). We also investigated the impact of main chain cyclic repeat units by synthesizing an analog with a linear oligosilane lacking stereogenic centers. We observed that stereoregular polysilanes exhibited more pronounced phase transition behaviors in DSC measurements and had more distinct absorption bands in the UV-vis spectra compared to atactic polysilanes. Influence of silane structures (cyclic *versus* linear) and vinyl group incorporation on the polysilane properties was also examined. Organosilicon materials containing hybrid σ,π-conjugated structures have raised broad interest for their unique optoelectronic properties and potential applications in photoresists, emitting polymers and semiconductive materials.

Experimental

Kumada polycondensation of di(bromothienyl)silane and aryl dibromide building blocks

In a glove box, an oven-dried 2-dram vial with stir bar was charged with di(bromothienyl)silane (1.0 equiv.) and THF (75 mM). *i*-PrMgCl (2.0 M in THF, 2.0 equiv.) was added by micro syringe. The solution was stirred at room temperature for 30 minutes, yielding a di-magnesio intermediate. $NidpppCl_2$ (0.1 equiv.), triphenylphosphine (0.2 equiv.) and aryl dibromide (1.5 equiv.) were weighed in a 2-dram vial with stir bar and dissolved in THF (0.3 mM). The solution of the di-magnesio intermediate was quickly added to the reaction mixture by pipette, yielding a dark red solution. Additional THF (0.3 mM) was used to rinse the vial and combined with the reaction mixture. The reaction was heated to 40 °C and allowed to stir for 24 hours in a glove box. After 24 hours, the reaction was quenched by adding the orange solution dropwise to 15 mL of dry methanol, which was stirred fast in a round bottom flask. Formation of precipitates was observed. The suspension was allowed to sit overnight, and the top clear yellow solution was removed. 10 mL of methanol were added, and precipitates were washed sufficiently by stirring vigorously for 30 minutes. The suspension was allowed to sit until the precipitates settled at the bottom. The above washing procedure was repeated 2 more times. Then the suspension was filtered through a Buchner funnel. The solid was washed with methanol and dried under vacuum, yielding hybrid polysilane products.

Results and discussion

Stereoregular hybrid σ,π-conjugated polymers

We previously reported the copolymerization of the building block *trans*-**1** and 2,5-dibromothiophene (Table 1, entry 1).[47] The building block *trans*-**1**, isolated in high diastereomeric purity after recrystallization, can be elaborated to conjugated polymer **P1** by Mg/Br exchange[52,53] followed by $NiCl_2$dppp-catalyzed Kumada polycondensation in the presence of PPh_3 ligands (Table 1, entry 1). Herein, the reaction conditions were further investigated by varying catalyst and ligand species (Table 1). At this time, the focus continued to be on Ni-catalyzed Kumada polycondensation as Ni does not cleave Si–Si bonds, whereas the Pd catalysts employed in Stille or Suzuki polycondensation are known to cleave Si–Si bonds.[54–56]

Under the $NiCl_2$dppp-catalyzed conditions, low conversions of starting materials were observed with no additional ligands (Table 1, entry 2). Although excess ligands are not usually

Table 1 Variation of **P1** yields with Ni catalysts and ligands

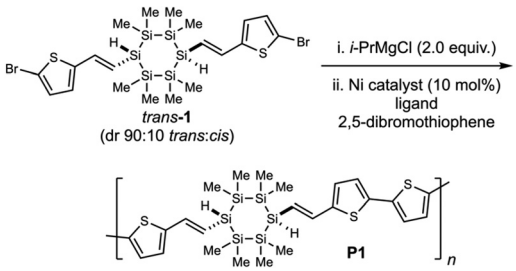

Entry	Catalyst	Ligand	Yield (%)
1[a]	$NiCl_2$dppp	PPh_3	78
2	$NiCl_2$dppp	n/a	Low
3	$NiCl_2$dppp	dppp	Low
4	$NiCl_2(PPh_3)_2$	PPh_3	63
5	$NiCl_2(PPh_3)_2$	n/a	65
6	$NiCl_2(PPh_3)_2$	dppp	55

[a] Previously reported in reference.[47]

required in the Kumada catalyst-transfer polycondensation (KCTP) towards poly(3-hexylthiophene),[57] similarly low yields were reported in Kumada couplings of heteroaryl chlorides and lithium tri(quinolyl)magnesates catalyzed by $Ni(acac)_2$ and dppp.[58] The low conversions might arise from a different copolymerization mechanism rather than KCTP. The cyclosilane building blocks lacked a continuous π-conjugated backbone, and prevented the Ni catalyst from "walking" along the polymer chain.[57] Therefore, the catalyst required regeneration after a growth of each unit. PPh_3 ligand might improve catalyst recovery and therefore result in a higher conversion of monomers. Further experimental exploration supported the above hypothesis. Additional dppp ligands did not improve the polymerization (Table 1, entry 3). Reasonable starting material conversion and molecular weight characteristics of products were observed in $NiCl_2(PPh_3)_2$-catalyzed polymerizations regardless of the ligand species and amount (Table 1, entries 4–6). The reaction condition described in Table 1, entry 1 was chosen as the general polymerization condition because of the relatively high conversion.

Under the optimized polymerization condition, we have now synthesized the stereoisomers of **P1** (Scheme 1 and Table 1) by variation of the diastereomeric ratio in the starting monomer **1**, yielding **P2** (predominantly *cis*) and **P3** (atactic) (Table 2). We note that *cis*-**1** (dr 20 : 80 *trans* : *cis*) was enriched in the filtrate obtained from recrystallization of **1**. Lower isolated yield in the synthesis of **P3** was attributed to a smaller reaction scale. The polymers **P2** and **P3** were insufficiently soluble in THF for SEC analysis. M_w values were instead assessed *via* diffusion-ordered NMR spectroscopy (DOSY) in $CDCl_3$ (Table 2).[59,60] Limited solubility was observed even in $CDCl_3$ (Fig. S2†). Molecular weight determination by DOSY cannot provide information about M_n or dispersity, however, there is no reason to think that these molecular weight characteristics would not be consistent with previously published **P1**.

Si–H functional groups are known to have distinctive resonances by both ^1H and ^{29}Si NMR spectroscopy,[22,23,46] and the comparison of ^{29}Si NMR spectra of cyclosilane monomers to polysilanes identified the retention of configuration in cyclosilane units during the copolymerization. The *Si*H resonances of cyclosilane conformers had distinct chemical shifts in ^{29}Si NMR spectra: −64.5 ppm for *trans*-**1** and −63.0 ppm for *cis*-**1** (Fig. 2). Polysilanes **P1-3** had similar *Si*H resonances compared to the monomers. Distinct peaks were found at −63.0 and/or −64.8 ppm depending on the diastereomer ratio of their start-

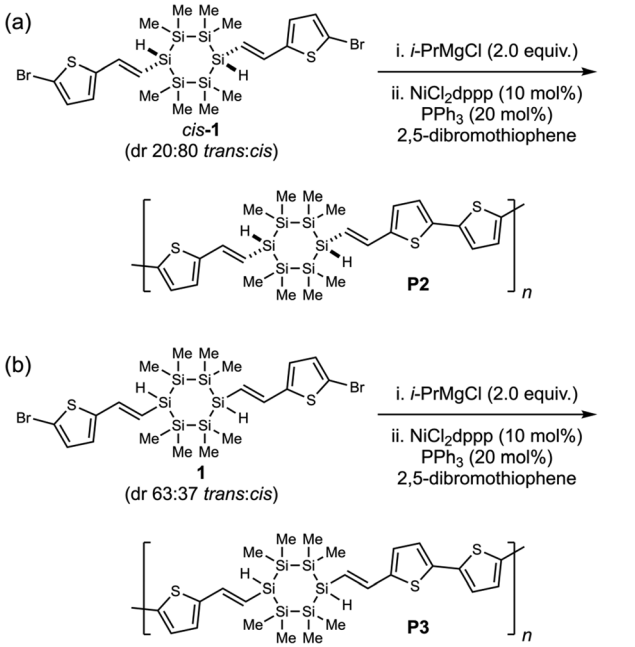

Scheme 1 Synthesis of hybrid conjugated polymers (a) **P2** (predominately *cis*) and (b) **P3** (atactic).

Table 2 Yields and molecular weight characteristics of hybrid conjugated polysilanes

Cyclosilane	dr (*trans* : *cis*)	Polymer	M_n (kDa)	M_w (kDa)	M_w/M_n	Yield (%)
trans-**1**[a]	90 : 10	**P1**	6.70[b]	17.6[b]	2.63[b]	78
cis-**1**	20 : 80	**P2**	N/A	57.6[c]	N/A	61
1	63 : 37	**P3**	N/A	24.3[c]	N/A	22

[a] Previously reported.[47] [b] Determined by size exclusion chromatography relative to polystyrene standards at 254 nm (THF, [copolymer] = 1 mg mL^{-1}, 40 °C, 0.35 mL min^{-1}, 10 μL injection). [c] Determined by diffusion-ordered spectroscopy relative to polystyrene standards ($CDCl_3$, [copolymer] = 0.5 mg mL^{-1}), for calibration curve see Fig. S3.†

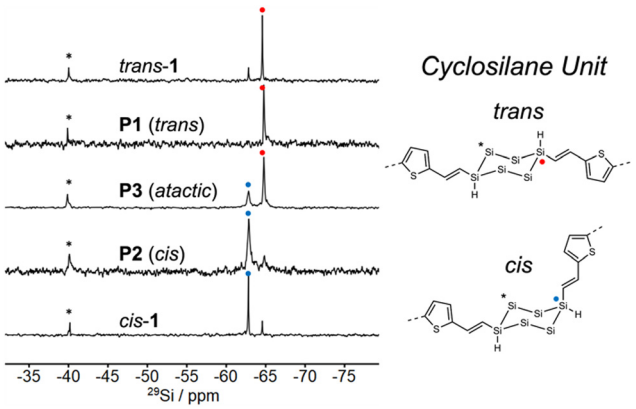

Fig. 2 Cropped ^{29}Si {^{1}H} DEPT spectra (79 MHz, $CDCl_3$) comparing (top to bottom) *trans*-**1** (dr 90 : 10 *trans* : *cis*), **P1**, **P3**, **P2** and *cis*-**1** (dr 20 : 80 *trans* : *cis*). $^{1}J_{Si-H}$ = 120 Hz. DEPT = distortionless enhancement by polarization transfer. The methyl groups are omitted for clarity.

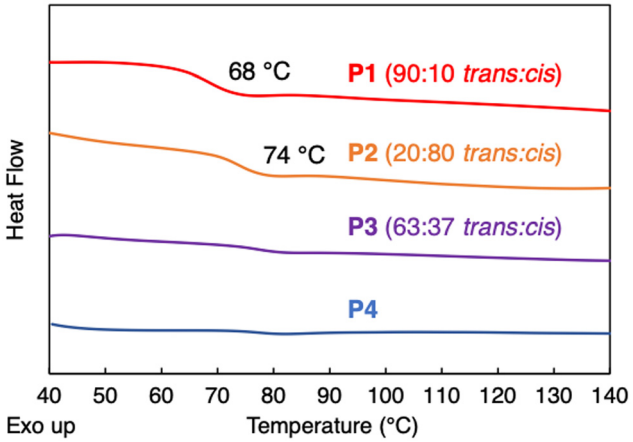

Fig. 3 Cropped DSC curves of **P1–4**. The second cycle is shown. Heating rate: 3 °C min^{-1}, cooling rate: 20 °C min^{-1}.

ing cyclosilanes. These features confirmed retention of configuration in the cyclosilane rings and that no Si–Si bond cleavage occurred in the Ni-catalyzed polycondensation.

Hybrid conjugated polymers containing linear silane units

To address the effect of cyclosilane units on the conjugated polymer properties, polysilane **P4** was synthesized as a comparison on the thermal and optical properties (Scheme 2). **P4** is similar to a known polymer bearing ethyl substituents on silicon.[49] The stoichiometric Mg/Br exchange of one Br group on 2,5-dibromothiophene was conducted at −78 °C in diethyl ether. Then the bromothienyl magnesium chloride was coupled to dichlorodisilane, affording **2**. The linear silane **2** was copolymerized with 2,5-dibromothiophene following the standard procedure, resulting in light orange powder **P4**.

Thermal properties *via* differential scanning calorimetry

The polymer glass transition temperature (T_g) is tacticity-dependent.[61,62] By achieving control of both relative configuration and molecular weight, it is possible to study the impact of tacticity on polymer properties in isolation. As an example of stereoregularity impact on bulk properties, we found that the three macromolecules exhibited distinct glass transition (T_g) temperatures. The atactic **P3** showed a minimal transition, but both *trans* **P1** and *cis* **P2** showed more pronounced T_g at

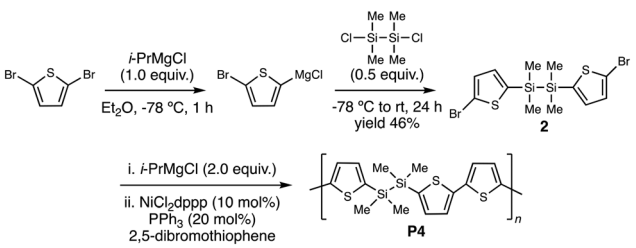

Scheme 2 Synthesis of hybrid conjugated polymer **P4** from a linear oligosilane **2** by Grignard reaction.

different temperatures (Fig. 3). Linear silane-embedded **P4** did not undergo a noticeable phase transition between 40 to 180 °C. The thermal property of atactic **P3** is consistent with the absence of a phase transition between 40 °C to 200 °C for atactic linear poly(cyclosilane)s.[29] It is somewhat surprising that *cis* **P2** should have a higher T_g than *trans* **P1**, as it might be expected that a *cis* relationship on a chair cyclohexasilane would result in greater free volume. We suggest that these data might support the possibility that in the solid state, the cyclohexasilane in a *cis* isomer adopts a more compact twist conformation, which has been seen in some crystal structures of cyclosilanes.[63]

To confirm the feasibility of this hypothesis, we calculated the energy of different conformations of *cis*-**1** in the gas phase at the B3LYP-D3(BJ)/6-311++G(d,p) level of theory (Fig. S4†). Multiple low-energy rotamers of the thiophene side chain were observed, as well as both the chair and twist-boat ring conformers. While most chair conformations were lower energy than twist-boat conformations, the magnitude of the energy difference varied between −1.16 kcal mol^{-1} and 5.96 kcal mol^{-1}, with one twist-boat rotamer being lower energy than an available chair conformation. Structural representations of the twist-boat conformations were more compact than the corresponding chair conformers. Similar trends were observed for H-*cis*-**1**, an analog of **1** without bromination (Fig. S5†). These data indicate that compounds structurally similar to the constitutional repeat unit of **P1** have multiple low energy conformations, which suggests that in the glassy state adoption of the more compact conformation could be feasible.

UV-vis absorbance spectra

We obtained UV-vis spectra of the stereoregular polysilane thin films. The polysilanes were dissolved in THF (2.0 mg mL^{-1}), drop-casted on quartz substrates and fully dried under vacuum at room temperature overnight (Fig. 4, blue curves). All three polymers were similar in UV-vis absorption: λ_{max} = *ca.* 420 nm and λ_{onset} = *ca.* 570 nm. No notable difference was identified,

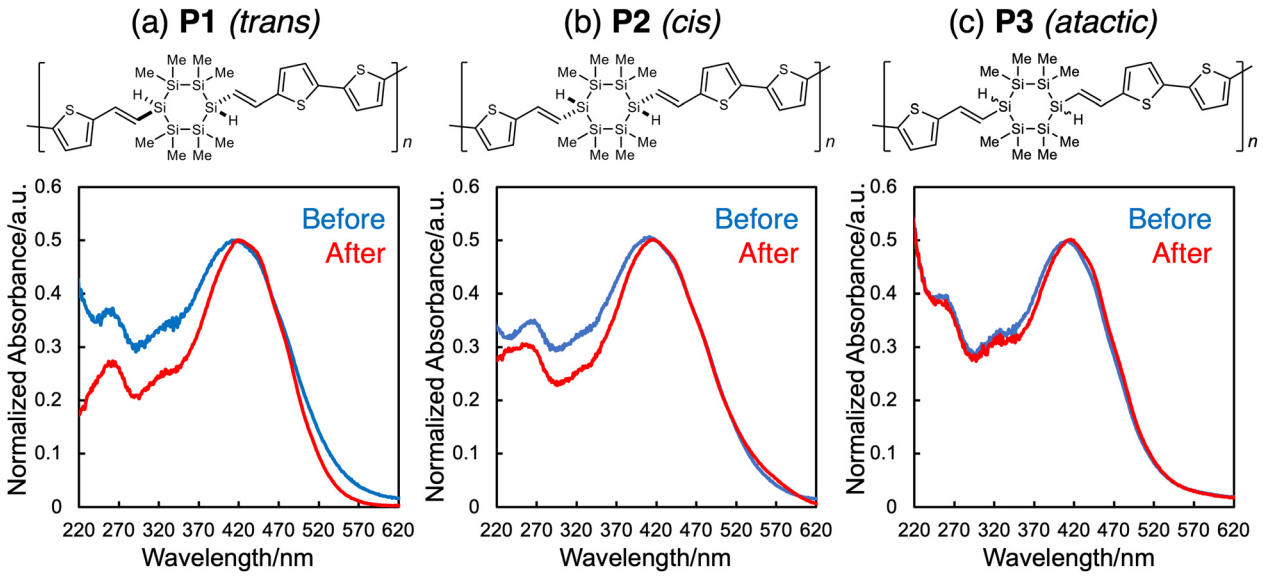

Fig. 4 Comparison of film UV-vis spectra of (a) **P1**, (b) **P2** and (c) **P3**. Before annealing: blue. After annealing: red.

which agreed with the similar UV-vis absorption of *trans*- and *cis*-**1**.

The films were then annealed by heating at 80 °C for 8 hours under vacuum and slowly cooled to room temperature overnight. Compared to UV-vis spectra obtained before annealing, all three annealed polymers showed similar onset (λ_{onset}) and maximum (λ_{max}) absorption, whereas the absorption bands became narrower only in spectra of annealed **P1** and **P2**. This is consistent with the DSC results that glass transition were observed in stereoregular polymers (**P1** and **P2**) but not atactic **P3**. Annealing the stereoregular polymers at temperature above T_g helped form more ordered arrangement of neighboring polymer chains, resulting in more distinct absorption bands.

We also evaluated solution-phase spectra of **P4** and **P1**, to determine if the cyclosilane impacted light absorption relative to linear silanes. There was a significant difference in λ_{max} observed between **P4** and **P1**, red-shifting from *ca.* 380 nm to *ca.* 420 nm, respectively (Fig. 5). This indicates an extension of conjugation with the incorporation of cyclosilane units and vinyl groups in the hybrid σ,π- conjugated structure.

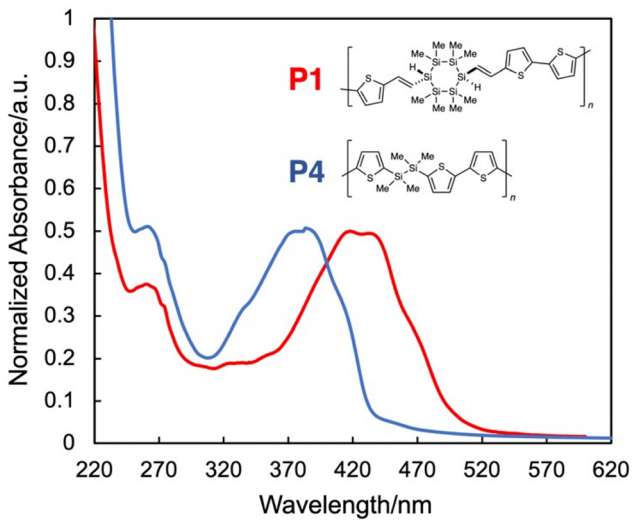

Fig. 5 Comparison of solution UV-vis spectra of **P1** (red) and **P4** (blue) in THF. [polymer] = 0.03 g L^{-1}.

Table 3 Yields of **P5** and **P6**

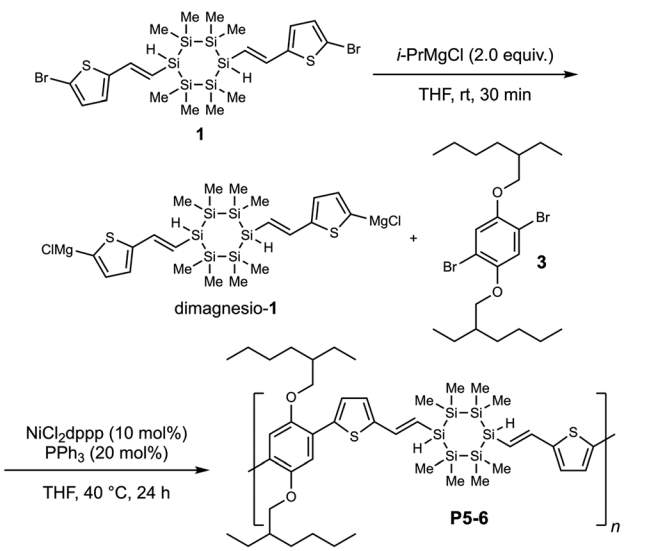

Cyclosilane	dr (*trans* : *cis*)	Polymer	Yield (%)
trans-**1**	90 : 10	**P5**	24
1	63 : 37	**P6**	35

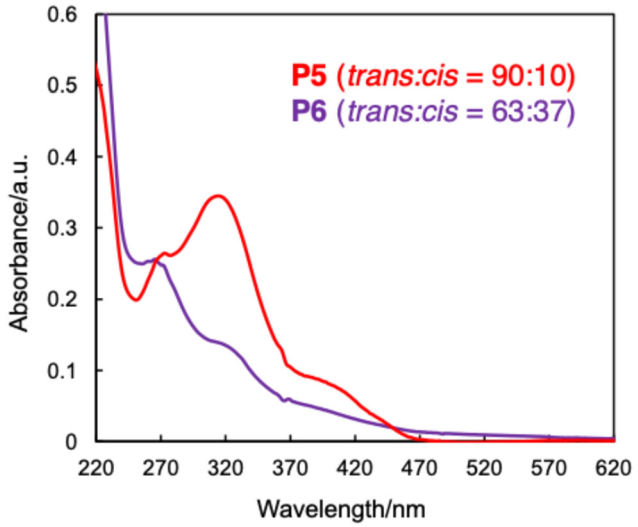

Fig. 6 Comparison of UV-vis spectra of **P5** (*trans*, red) and **P6** (atactic, purple) in THF solution. [polymer] = 0.03 g L^{-1}.

Expanded scope of hybrid conjugated polymers

To further investigate the scope of the copolymerization and stereoregularity, we replaced the comonomer 2,5-dibromothiophene with arene **3** (synthesized according to published procedure[64]) to form conjugated polymers **P5** and **P6** (Table 3). Limited solubility in both THF and $CDCl_3$ (Fig. S2†) prevented molecular weight analysis by GPC or DOSY. As the *trans* : *cis* ratio in **1** tuned from 90 : 10 to 63 : 37, the yields of the copolymers stayed consistent (Table 3), but significantly different absorbance spectra were recorded (Fig. 6). Increasing the ratio of a certain diastereomer of cyclosilane led to a more pronounced transition at *ca.* 320 nm and a more notable shoulder at 370 nm (Fig. 6).

Conclusions

We demonstrated that stereoregularity showed substantial influence on the thermal and optical properties of hybrid conjugated polymers. A series of stereoregular and atactic σ,π-conjugated polymers derived from sterically pre-defined cyclosilane building blocks were synthesized. Compared to the atactic polymer, the stereoregular polysilanes exhibited notable phase transitions and their optical characteristics better benefitted from annealing. Using blocky aromatic comonomers, the impact of stereoregularity on the optical properties was amplified and the absorption features were more distinct in the solution phase. We also demonstrated that the incorporation of cyclosilane and vinyl units into the polymer chain extended conjugation.

This overall approach yields examples of highly stereoregular polysilanes, which remain rare in the literature. Both the synthesis and assignment were possible due to the synthesis of well-defined small molecules, which served as both analytical comparisons and as building blocks.

Conflicts of interest

There are no conflicts to declare.

Data availability

The data supporting this article have been included as part of the ESI.†

Acknowledgements

This research was primarily supported by the U.S. Department of Energy (DOE), Office of Science, Basic Energy Sciences, under Award No. DE-SC0020681.

References

1 J. C. Worch, H. Prydderch, S. Jimaja, P. Bexis, M. L. Becker and A. P. Dove, *Nat. Rev. Chem.*, 2019, **3**, 514–535.
2 G. W. Coates, *Chem. Rev.*, 2000, **100**, 1223–1252.
3 J. Szejtli, *Chem. Rev.*, 1998, **98**, 1743–1754.
4 J. Wang, J. Zhou, Y. Ding, X. Hu and Y. Chen, *Polym. Chem.*, 2023, **14**, 2414–2434.
5 L. Wu, Z. Zhou, D. Sathe, J. Zhou, S. Dym, Z. Zhao, J. Wang and J. Niu, *Nat. Chem.*, 2023, **15**, 1276–1284.
6 L. M. Lillie, W. B. Tolman and T. M. Reineke, *Polym. Chem.*, 2017, **8**, 3746–3754.
7 M. K. Porwal, Y. Reddi, D. J. Saxon, C. J. Cramer, C. J. Ellison and T. M. Reineke, *Chem. Sci.*, 2022, **13**, 4512–4522.
8 C. J. Stubbs, J. C. Worch, H. Prydderch, Z. Wang, R. T. Mathers, A. V. Dobrynin, M. L. Becker and A. P. Dove, *J. Am. Chem. Soc.*, 2022, **144**, 1243–1250.
9 M. K. Stanfield, R. S. Terry, J. A. Smith and S. C. Thickett, *Polym. Chem.*, 2023, **14**, 4949–4956.
10 R. J. Kieber, C. Ozkardes, N. Sanchez and J. G. Kennemur, *Polym. Chem.*, 2019, **10**, 3514–3524.
11 M. Piccini, D. J. Leak, C. J. Chuck and A. Buchard, *Polym. Chem.*, 2020, **11**, 2681–2691.
12 K. E. Crawford and L. R. Sita, *J. Am. Chem. Soc.*, 2013, **135**, 8778–8781.
13 K. E. Crawford and L. R. Sita, *ACS Macro Lett.*, 2014, **3**, 506–509.
14 H. Wang, Y. Zhao, M. Nishiura, Y. Yang, G. Luo, Y. Luo and Z. Hou, *J. Am. Chem. Soc.*, 2019, **141**, 12624–12633.
15 D. Takeuchi, *J. Am. Chem. Soc.*, 2011, **133**, 11106–11109.
16 D. Pasini and D. Takeuchi, *Chem. Rev.*, 2018, **118**, 8983–9057.
17 J. Zhu and E. Y.-X. Chen, *Angew. Chem., Int. Ed.*, 2018, **57**, 12558–12562.
18 B. Han, L. Zhang, B. Liu, X. Dong, I. Kim, Z. Duan and P. Theato, *Macromolecules*, 2015, **48**, 3431–3437.

19 D. Sathe, J. Zhou, H. Chen, H.-W. Su, W. Xie, T.-G. Hsu, B. R. Schrage, T. Smith, C. J. Ziegler and J. Wang, *Nat. Chem.*, 2021, **13**, 743–750.
20 R. R. Schrock, *Acc. Chem. Res.*, 2014, **47**, 2457–2466.
21 S.-Y. Shan, W. Zhang, Q. Cao, Y.-C. Ye, Z. Cai and J.-B. Zhu, *Polym. Chem.*, 2024, **15**, 1070–1076.
22 E. M. Press, E. A. Marro, S. K. Surampudi, M. A. Siegler, J. A. Tang and R. S. Klausen, *Angew. Chem., Int. Ed.*, 2017, **56**, 568–572.
23 E. A. Marro, E. M. Press, M. A. Siegler and R. S. Klausen, *J. Am. Chem. Soc.*, 2018, **140**, 5976–5986.
24 C. P. Folster and R. S. Klausen, *Polym. Chem.*, 2018, **9**, 1938–1941.
25 E. A. Marro and R. S. Klausen, *Chem. Mater.*, 2019, **31**, 2202–2211.
26 Q. Jiang, S. Wong and R. S. Klausen, *Polym. Chem.*, 2021, **12**, 4785–4794.
27 F. Fang, Q. Jiang and R. S. Klausen, *J. Am. Chem. Soc.*, 2022, **144**, 7834–7843.
28 M. G. Coschigano, S. L. Gregory, J. Catazaro, A. J. Rossini and R. S. Klausen, *Macromolecules*, 2024, **57**, 4095–4106.
29 R. W. Dorn, E. A. Marro, M. P. Hanrahan, R. S. Klausen and A. J. Rossini, *Chem. Mater.*, 2019, **31**, 9168–9178.
30 F. C. Schilling, F. A. Bovey and J. M. Zeigler, *Macromolecules*, 1986, **19**, 2309–2312.
31 A. R. Wolff, J. Maxka and R. West, *J. Polym. Sci., Part A: Polym. Chem.*, 1988, **26**, 713–720.
32 A. R. Wolff, I. Nozue, J. Maxka and R. West, *J. Polym. Sci., Part A: Polym. Chem.*, 1988, **26**, 701–712.
33 J. Maxka, F. K. Mitter, D. R. Powell and R. West, *Organometallics*, 1991, **10**, 660–664.
34 K. E. Wentz, A. F. Gittens and R. S. Klausen, *J. Am. Chem. Soc.*, 2025, **147**, 2938–2959.
35 T. Moritani, I. Kuruma, K. Shibatani and Y. Fujiwara, *Macromolecules*, 1972, **5**, 577–580.
36 A. E. Tonelli and F. C. Schilling, *Acc. Chem. Res.*, 1981, **14**, 233–238.
37 J. P. Banovetz, K. M. Stein and R. M. Waymouth, *Organometallics*, 1991, **10**, 3430–3432.
38 N. Choi, S. Onozawa, T. Sakakura and M. Tanaka, *Organometallics*, 1997, **16**, 2765–2767.
39 B. J. Grimmond and J. Y. Corey, *Organometallics*, 1999, **18**, 2223–2229.
40 B. J. Grimmond and J. Y. Corey, *Organometallics*, 2000, **19**, 3776–3783.
41 V. K. Dioumaev, K. Rahimian, F. Gauvin and J. F. Harrod, *Organometallics*, 1999, **18**, 2249–2255.
42 E. Fossum and K. Matyjaszewski, *Macromolecules*, 1995, **28**, 1618–1625.
43 E. Fossum, S. W. Gordon-Wylie and K. Matyjaszewski, *Organometallics*, 1994, **13**, 1695–1698.
44 H. Sakurai, R. Honbori and T. Sanji, *Organometallics*, 2005, **24**, 4119–4121.
45 E. A. Marro, C. P. Folster, E. M. Press, H. Im, J. T. Ferguson, M. A. Siegler and R. S. Klausen, *J. Am. Chem. Soc.*, 2019, **141**, 17926–17936.
46 J. T. Ferguson, Q. Jiang, E. A. Marro, M. A. Siegler and R. S. Klausen, *Dalton Trans.*, 2020, **49**, 14951–14961.
47 Q. Jiang, A. F. Gittens, S. Wong, M. A. Siegler and R. S. Klausen, *Chem. Sci.*, 2022, **13**, 7587–7593.
48 K. Kanno, Y. Aikawa and S. Kyushin, *Tetrahedron Lett.*, 2020, **61**, 152274.
49 A. Kunai, T. Ueda, K. Horata, E. Toyoda, I. Nagamoto, J. Ohshita, M. Ishikawa and K. Tanaka, *Organometallics*, 1996, **15**, 2000–2008.
50 J. Ohshita, D. Kanaya, M. Ishikawa, T. Koike and T. Yamanaka, *Macromolecules*, 1991, **24**, 2106–2107.
51 J. Ohshita, Y. Matsuzawa, T. Yagami, Y. Adachi, A. Sekiguchi, M. Ohashi and H. Nakano, *Chem. Lett.*, 2020, **49**, 1174–1177.
52 P. Knochel, W. Dohle, N. Gommermann, F. F. Kneisel, F. Kopp, T. Korn, I. Sapountzis and V. A. Vu, *Angew. Chem., Int. Ed.*, 2003, **42**, 4302–4320.
53 A. Krasovskiy and P. Knochel, *Angew. Chem., Int. Ed.*, 2004, **43**, 3333–3336.
54 K. Yamamoto, M. Kumada, I. Nakajima, K. Maeda and N. Imaki, *J. Organomet. Chem.*, 1968, **13**, 329–341.
55 H. K. Sharma and K. H. Pannell, *Chem. Rev.*, 1995, **95**, 1351–1374.
56 H. Yamashita, N. P. Reddy and M. Tanaka, *Macromolecules*, 1993, **26**, 2143–2144.
57 T. Beryozkina, V. Senkovskyy, E. Kaul and A. Kiriy, *Macromolecules*, 2008, **41**, 7817–7823.
58 S. Dumouchel, F. Mongin, F. Trécourt and G. Quéguiner, *Tetrahedron*, 2003, **59**, 8629–8640.
59 W. Li, H. Chung, C. Daeffler, J. A. Johnson and R. H. Grubbs, *Macromolecules*, 2012, **45**, 9595–9603.
60 K. Gu, J. Onorato, S. S. Xiao, C. K. Luscombe and Y.-L. Loo, *Chem. Mater.*, 2018, **30**, 570–576.
61 E. V. Thompson, *J. Polym. Sci., Part A-2*, 1966, **4**, 199–208.
62 L. Chang and E. M. Woo, *Polym. Chem.*, 2010, **1**, 198–202.
63 A. F. Gittens, Q. Jiang, M. A. Siegler and R. S. Klausen, *Organometallics*, 2022, **41**, 3762–3769.
64 A. P. Monkman, L.-O. Palsson, R. W. T. Higgins, C. Wang, M. R. Bryce, A. S. Batsanov and J. A. K. Howard, *J. Am. Chem. Soc.*, 2002, **124**, 6049–6055.